

An experimental study on the development of ultra-high strength powder concrete using ferro-silicon

Byung-Wan Jo, Kwang-Won Yoon*, Ji-Sun Choi and Jung-Hoon Park

Dept. of Civil Engineering, Hanyang University, Seoul, South Korea.

In this study, ordinary and low-heat Portland cement and ordinary Portland cement were used for experiments and the air gap was minimized by using minute quartz as a filling. Additionally, a steel fiber was used to solve the brittle failure problem observed at high-intensity stresses. This study aimed to make an ultra-high strength powdered concrete, which has a compressive strength above 400 MPa. Ultra-high strength powdered concrete, which is different from the original concrete, is highly influenced by the materials used. In the study, the following had an effect on the compressive strength: ferro silicon > bauxite > dolomite > silicon. According to the SEM results, C-S-H hydrate was made in the highest quantity, and tobermorite and zonalite were made by high temperature and pressure curing, respectively. In this study, ultra-high strength powdered concrete, which has a 28th day compressive strength of 420 MPa, has been successfully made.

Key words: Ultra-high strength powder concrete, Ferro-silicon, Low heat Portland cement, Transition zone, High temperature, High pressure curing.

Introduction

As buildings tend to become extremely tall, large, and of special design or purpose, high performance construction materials are needed. Concrete is widely used as an important and excellent construction material in terms of economic efficiency and durability, together with steels. Specifically, high-strength concrete can be used in light-weight, large, high-storied, and efficient spatial building construction because of reduced sections and lowered self-weight. Considering these properties, it may be a beneficial construction material in terms of earthquake resistance and durability. Therefore, it is necessary to develop an ultra-high strength concrete maximizing the strength of existing concretes by use of proper admixtures, mixtures, manufacturing, and curing methods [1]. The methods of preparing ultra-high strength concrete are classified into strengthening cement paste, strengthening the aggregate, and strengthening the bond strength of the aggregate and binder; for this, selecting improved aggregates, reducing the water-cement ratio, improving the curing method, and using an admixture or a high performance water reducing agent is recommended.

In this study to develop ultra-high strength powder concrete, each component of concrete, aggregates, and cement were considered and the compressive strength was compared, in order to obtain a compressive strength

of 400 MPa or higher- the highest level in the territory [2-3]. In addition, silica fume, minute quartz, fiber reinforcement, and the types, input ratio, and curing methods of the cement in the powder concrete were selected as variables to evaluate their impact on manufacturing ultra-high strength powder concrete [4]. The internal structure was analyzed by SEM and XRD analysis.

Research Significance

Recently, buildings and structures are becoming quite tall and large, and some large construction companies are actively planning to construct skyscrapers of over 100 stories. These buildings require high performance construction materials. Therefore, it is necessary to develop an ultra-high strength concrete by use of proper admixture, mixture, manufacturing, and curing methods. We think that our data could be of considerable help in the process of establishing high performance construction materials.

Experimental Procedure

Materials

Cement

The study used low heat Portland cement and ordinary Portland cement, and Tables 1 and 2 show the mineral compositions and chemical/physical properties of such cements [5-6].

Quartz sand

The study used quartz sand consisting of quartz granules containing SiO₂. The study used sintered sand,

*Corresponding author:
Tel : 02-2220-0327
Fax: 02-2292-0321
E-mail: ykwabc@nate.com

Table 1. Low heat Portland cement

Items		component ratio
Mineralogical Composition, weight %	C ₃ S (3CaO·SiO ₂)	31
	C ₂ S (2CaO·SiO ₂)	48
	C ₃ A (3CaO·Al ₂ O ₃)	3
	C ₄ AF(4CaO·Fe ₂ O ₃ ·Al ₂ O ₃)	11
Chemical Composition, weight %	Calcium oxide (CaO)	62.5
	Silicon dioxide (SiO ₂)	25.3
	Aluminium oxide (Al ₂ O ₃)	3.1
	Ferric oxide (Fe ₂ O ₃)	3.6
	Sulfur trioxide (SO ₃)	2.3
	Loss on ignition	2.0
Physical properties	Specific gravity, g/cm ³	3.22

Table 2. Ordinary Portland cement

Items		component ratio
Mineralogical Composition, weight %	C ₃ S (3CaO·SiO ₂)	49
	C ₂ S (2CaO·SiO ₂)	23
	C ₃ A (3CaO·Al ₂ O ₃)	10
	C ₄ AF(4CaO·Fe ₂ O ₃ ·Al ₂ O ₃)	9
Chemical Composition, weight %	Calcium oxide (CaO)	62.5
	Silicon dioxide (SiO ₂)	21.0
	Aluminium oxide (Al ₂ O ₃)	5.9
	Ferric oxide (Fe ₂ O ₃)	3.2
	Sulfur trioxide (SO ₃)	2.1
Physical properties	Specific gravity, g/cm ³	3.15

Table 3. Physical properties of Quartz sand

Size, mm	specific gravity, g/cm ³	Unit weight, N/cm ²	Fineness modulus	Absorption, %
0.2~0.4	2.64	1,600	1.4~1.6	0.1

and Table 3 shows the physical properties

Dolomite

The chemical composition of dolomite used in this study is CaMg(CO₃)₂, in which calcium carbonate and magnesium carbonate are 1 : 1 mixed. Tables 4 and 5 show the chemical and physical properties of dolomite.

Bauxite

The bauxite used in the study was also used as an alumina source in the Portland cement or the main ingredient of the high alumina cement. Table 6 shows the physical/chemical properties of bauxite.

Ferro Silicon

The ferro silicon alloy used in the study, an electrical

Table 4. Chemical properties of dolomite

CaO	29 ~ 30%
MgO	20 ~ 21%
SiO ₂	0.5 ~ 1.5%
Fe ₂ O ₃	0.2 ~ 0.5%
Al ₂ O ₃	0.1 ~ 0.2%

Table 5. Physical properties of dolomite

Color	Milky white
Specific Gravity, g/cm ³	2.8 ~ 2.9
PH	9 ~ 10
Size, mm	0.6

Table 6. Physical-Chemical properties of Bauxite

Size, mm	fineness modulus	specific gravity, g/cm ³	the principal ingredient	Color
0.3	2.97	3.3	Al ₂ O ₃	Brown

Table 7. Chemical properties of Ferro Silicon (75%)

Items	Specification, %					Size, μm
	Si	C	S	P	Al	
Ferro Silicon	75	0.2	0.02	0.04	2.0	43

Table 8. Physical properties of minute quartz

Appearance (whiteness)	White powder (> 95)
Specific Gravity, g/cm ³	2.65
PH	7 ~ 8.5
Size, μm	4 ~ 15

steel, is used as the iron core in motors or transformers of motorized devices. as well as an electrical material with a high efficiency, especially in high speed motors, low noise transformers, and high frequency inductors [7]. Ferro silicon has an excellent tensile strength but few studies have reported its application as a cement binder. Table 7 shows the chemical properties of ferro silicon (75%).

Filler

To supplement insufficient SiO₂ to act as a filler by being filled into the transition zone between cement paste and aggregate to prevent transition zone destruction and improve strength, minute quartz was used as the filler [8]. Table 8 and 9 show the physical and chemical properties.

Fiber reinforcement

According to ASTM A 820-85, fiber reinforcement is classified into those: 1) cut along a cold extrusion line, 2) cut from a steel plate, and 3) extruded in a

Table 9. Chemical properties of minute quartz

SiO ₂ %	> 99.7	CaO%	Trace
Al ₂ O ₃ %	< 0.15	MgO%	Trace
Fe ₂ O ₃ %	< 0.03	H ₂ O%	< 0.05
TiO ₂ %	< 0.02		

Table 10. Physical properties of fiber reinforcement

Specific gravity, g/cm ³	Tensile strength, kgf/cm ²	Aspect Ratio	Flexural Toughness, %	Diameter, mm	Length, mm
7.86	9000~10000	60	> 68	0.5	30

Table 11. Chemical properties of high performance water reducing agent

Form	Specific gravity, g/cm ³	Ph	Color	Cl-content, %	Alkali content, %
Liquid	1.09	6.5 ± 1.0	Brown	≤ 0.01	≤ 0.2

Table 12. Proportions of ultra-high strength powder concrete

Cement	Aggregate	Classification	Cement	Minutely Quartz	Silica Fume	Steel Fiber	Aggregate	Mineral Admixture	W/C
Ordinary Portland cement	Quartz sand	QS05	1	0.35	0.2	0.3	0.5	0.043	0.15
		QS07	1	0.35	0.2	0.3	0.7	0.043	0.15
		QS09	1	0.35	0.2	0.3	0.9	0.043	0.15
		QS11	1	0.35	0.2	0.3	1.1	0.043	0.15
		QS13	1	0.35	0.2	0.3	1.3	0.043	0.15
	Dolomite	DOL05	1	0.35	0.2	0.3	0.7	0.043	0.15
		DOL07	1	0.35	0.2	0.3	0.7	0.043	0.15
		DOL09	1	0.35	0.2	0.3	0.9	0.043	0.15
		DOL11	1	0.35	0.2	0.3	1.1	0.043	0.15
	Bauxite	DOL13	1	0.35	0.2	0.3	1.3	0.043	0.15
		BX05	1	0.35	0.2	0.3	0.7	0.043	0.15
		BX07	1	0.35	0.2	0.3	0.7	0.043	0.15
		BX09	1	0.35	0.2	0.3	0.9	0.043	0.15
Ferro- silicon	Bauxite	BX11	1	0.35	0.2	0.3	1.1	0.043	0.15
		BX13	1	0.35	0.2	0.3	1.3	0.043	0.15
		OFS05	1	0.351	0.2	0.3	0.5	0.043	0.15
		OFS07	1	0.35	0.2	0.3	0.7	0.043	0.15
		OFS09	1	0.35	0.2	0.3	0.9	0.043	0.15
		OFS11	1	0.35	0.2	0.3	1.1	0.043	0.15
		OFS13	1	0.35	0.2	0.3	1.3	0.043	0.15
Low-heat Portland cement	Bauxite	BFS05	1	0.35	0.2	0.3	0.5	0.018	0.15
		BFS07	1	0.35	0.2	0.3	0.7	0.018	0.15
		BFS09	1	0.35	0.2	0.3	0.9	0.018	0.15
		BFS11	1	0.35	0.2	0.3	1.1	0.018	0.15
		BFS13	1	0.35	0.2	0.3	1.3	0.018	0.15

molten state, but to use in a high strength concrete, such a reinforcement should basically have: 1) a uniform dispersion in concrete, 2) a strong pullout resistance, and 3) a high tensile strength [9]. The fiber reinforcement utilized in this study was ASTM A 820 Type 1 (hooked-type round steel fiber). Table 10 shows the fiber's physical properties.

High performance water reducing agent

The basic mixture of high performance concrete necessitates the use of a water reducing agent as an admixture to secure proper workability, because a low water-cement ratio may cause poor workability. If adding a high performance water reducing agent to cement paste, the particles are absorbed onto specific surfaces, forming an electrified layer, a so called electrical double layer. Therefore, electrostatic resistance among particles corresponding to the charge of the electrical double layer occurs, thereby dispersing the cohesive particles and improving the fluidity of the

cement paste [10]. This study used a high performance water reducing agent; Table 11 shows its chemical properties.

Variable

Mixture

The mixture design in the study adopted a 15% water-cement ratio in the case of the ordinary Portland cement and a relatively low 16% ratio for the low heat Portland cement. Finally, the aggregates were mixed at 50%~130% by 20% increments on the basis of cement weight. Table 12 shows the mixture information.

Curing methods

Manufacturing ultra-high strength concrete requires a composite reaction of physical effects, like improving the fine structure, and chemical effects, like the hydration reaction and pozzolanic reaction. Therefore, to obtain higher strength concrete, the curing conditions were 20 °C water curing, 90 °C hydrothermal curing, and 250 °C-50 MPa high temp and high pressure curing as variables. An autoclave was used at high temperature to facilitate the pozzolanic reaction and the hydration reaction. Fig. 1 shows the high temperature and high pressure curing procedure.

Test methods

Specimen preparation

According to the mixture design of this study, aggregates, cement, admixture, and filler were sequentially put into a mixer with an eight capacity for dry mixing for two minutes each, and then mixed again with a high performance water reducing agent and mixing water

for eight minutes. Fig. 2 shows a diagram of high strength concrete mixing order.

Compressive Strength

To examine the changes of compressive strength depending on the effect of the variables, specimens were prepared in a 50*50*50 mm square pillar shaped mold. For every mixture, three specimens were used to measure the compressive strength and the average was used; the compressive strength was measured using KSL 5105 (compressive strength test method of hydraulic mortar).

Results and Discussion

Comparative analysis of compressive strength

To evaluate the compressive strength depending on types of aggregates, mixture, and curing temperature, specimens were prepared for each mixture and the curing was executed under 20 °C water curing, 90 °C hydrothermal curing, 250 °C-50 MPa high temp. and high pressure curing. The compressive strength was measured at day 7 and day 28. Table 13 shows the averages of three specimens per sample.

It was found that to obtain high strength concrete, selecting aggregates played a pivotal role. As seen in Fig. 3, when considering the compressive strength depending on aggregates, ferro silicon > bauxite > dolomite > silicon.

Considering the compressive strength by aggregate type, the input amounts were not identical and the

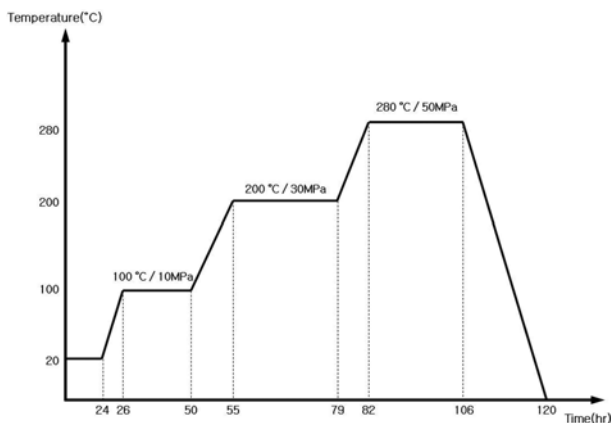


Fig. 1. Curing conditions

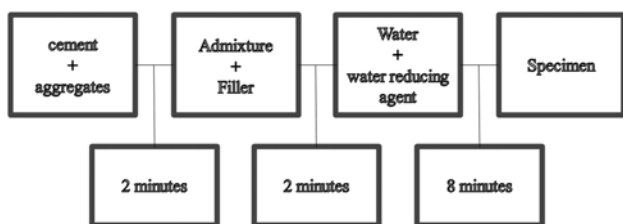


Fig. 2. Process of mixing

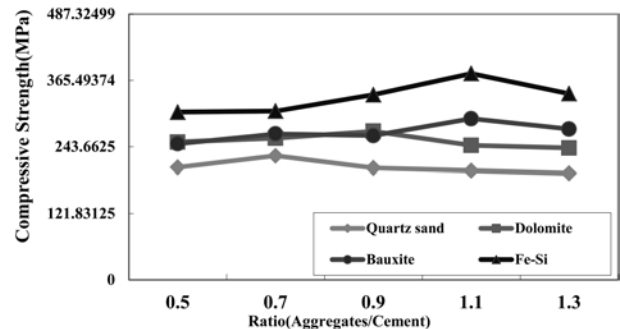


Fig. 3. Compressive strength of the aggregates at age (28 days)

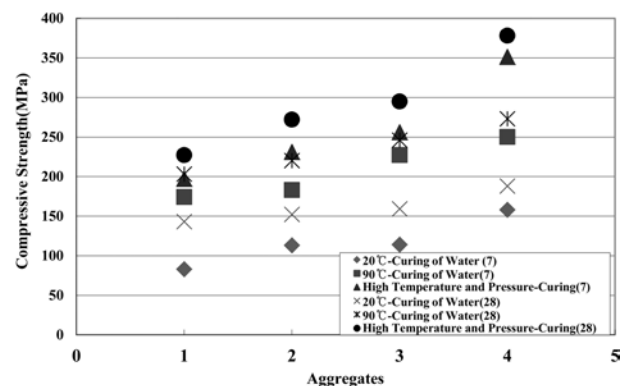


Fig. 4. Compressive strength of aggregates at various age

Table 13. Compressive strength by curing method

	Specimen	20 °C-Curing of Water		90 °C-Curing of Water		High Temperature and Pressure-Curing			
		Compressive Strength, MPa		Compressive Strength, MPa		Compressive Strength, MPa			
		7days	28days	7days	28days	7days	28days		
Ordinary Portland cement	Quartz sand	QS05	75	98	168	190	189	206	
		QS07	83	143	174	203	197	227	
		QS09	77	91	157	180	183	205	
		QS11	69	86	169	183	180	200	
		QS13	71	83	153	175	172	195	
		Dolomite	DOL05	92	131	163	190	216	252
			DOL07	98	120	169	201	227	259
			DOL09	113	152	183	220	231	272
			DOL11	88	119	150	191	202	246
			DOL13	89	124	153	188	207	241
		Bauxite	BX05	87	120	200	237	220	249
			BX07	109	134	198	239	224	267
			BX09	98	127	203	223	230	264
			BX11	114	159	227	246	256	295
			BX13	102	135	201	225	233	276
		Ferro-silicon	OFS05	127	158	220	237	290	307
			OFS07	136	141	215	249	295	309
			OFS09	147	148	231	260	327	339
			OFS11	158	188	250	273	351	378
			OFS13	139	153	237	268	323	341
Low-heat Portland cement	Ferro-silicon	BFS05	105	139	233	249	301	334	
		BFS07	119	140	240	260	310	342	
		BFS09	130	151	232	271	347	391	
		BFS11	142	160	290	315	379	420	
		BFS13	111	149	245	287	348	381	

highest compressive strength was found at aggregate-cement ratios of silicon 70%, dolomite 90%, and bauxite and ferro silicon 110%. In addition, the compressive strength increased as the amount of aggregate approaches the proper input ratio, but an excessive input ratio also reduced the strength.

The concrete strength increased by ageing. In the case of wet curing after concrete filling, 70% of the final strength was noted at day 28 and 85~90% at day 14. Fig. 4 shows the changes of compressive strength by ageing of each curing method, in which it was 72% in 20 °C water curing and 9% in both 90 °C hydrothermal curing and 250 °C-50 MPa high temp and high pressure curing, which may mean that the initial hydration reaction is highly activated in a high temperature environment higher than 90 °C, and then remains steady after day 7.

As seen in the results, it was found that the curing temperature and pressure improve the bonding between aggregates and generates hydrates, as well as forming a transitional area of cement hydrates [11].

If a fine powder like quartz was used in the study, it may react with calcium hydroxide, filling such pores and probably improving the strength.

Although ferro silicon demonstrated the highest compressive strength, the low heat Portland cement was compared to ordinary Portland cement. It showed that the specimen using low heat Portland cement had a lower strength at 20 °C water curing, but a higher compressive strength at temperatures greater than 100 °C. It seems that in case of 20 °C water curing, it might be attributable to belite cement of which the initial strength is low, but the long term strength is high. In the case of high temperature curing, 100 °C,

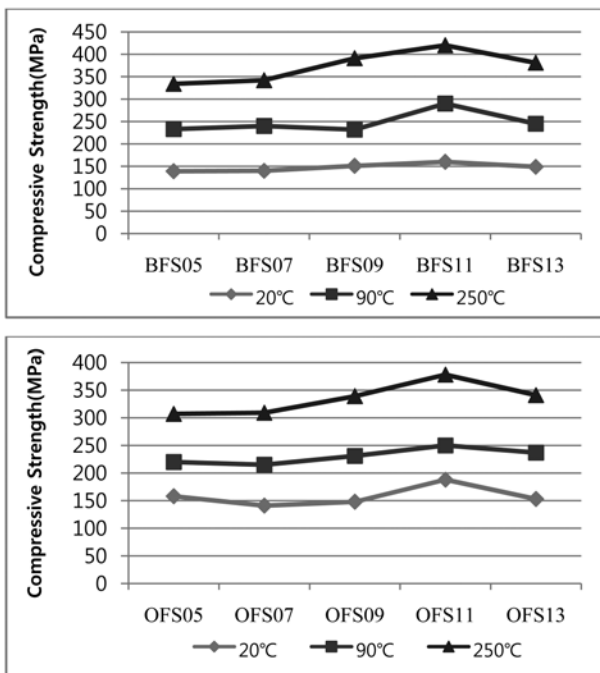


Fig. 5. Compressive strength of aggregates by the curing method (28 days)

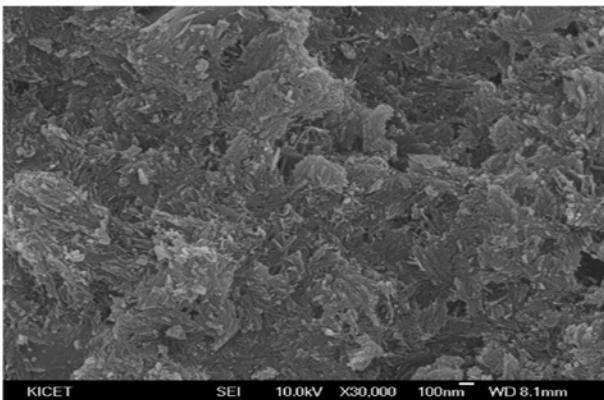


Fig. 6. SEM of the QS07 hydrate

using low heat Portland cement reduced the water-cement ratio, generating a more compactly hardened cement, facilitating hydration reaction, and finally improving the strength. Fig. 5 compares shows the compressive strength of each curing method. As the results show, the curing temperature and pressure increase the bonding between aggregates and hydrates, as well as forming a transitioning area of cement hydrates.

SEM image analysis

To explain the mechanism of the influence of ferro silicon on the strength, the internal structure of QS07 and BS11 was examined scanned by a scanning electron microscope (SEM) at day 7, to evaluate the hydrate generation and fine structure. If Portland cement is completely hydrated, calcium hydroxide accounts for 20~30%. The chemical composition is $\text{Ca}(\text{OH})_2$, showing a stratiform structure of uniform

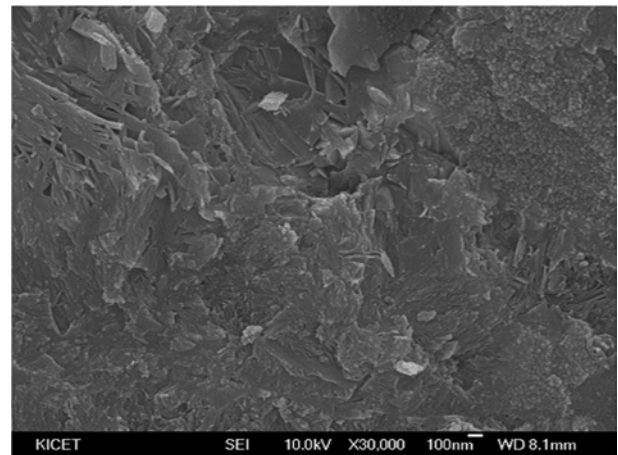


Fig. 7. SEM of the FS11 hydrate

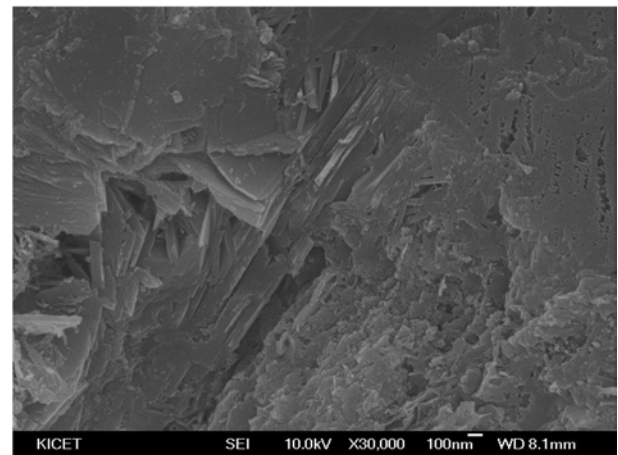


Fig. 8. SEM of the OFS11 hydrate

crystal compounds; the calcium atom is octahedral incoordination, while the oxygen atom has a tetrahedral coordination with a weak stratiform bond, which may cause a lowered chemical resistance and water permeability. As Fig. 6 shows, the ordinary Portland cement concrete has independently formed a C-S-H gel, mutually linked acicular hydrates (ettringite), and many $\text{Ca}(\text{OH})_2$ crystals, showing a sparse internal structure with non-crystal hydrates. Fig. 7 shows an image of the internal hydrates of the ultra-high strength powder concrete using ferro silicon taken by an SEM. The hardened structure of the ultra-high strength powder concrete was somewhat compactly structured with few $\text{Ca}(\text{OH})_2$ crystals, which may be attributable to the facilitated pozzolanic reaction when ferrosilicon powder was cured under a high temperature and high pressure, thus forming a C-S-H gel [12]. It also showed that the hardened structure is more compact than the ordinary Portland cement concrete. In addition, it shows uniformly distributed hydrate products throughout the concrete, which is probably attributable to forming various hydrates such as C-S-H¹, C-A-H² when the pozzolanic reaction was facilitated by using ferro silicon, an admixture, and

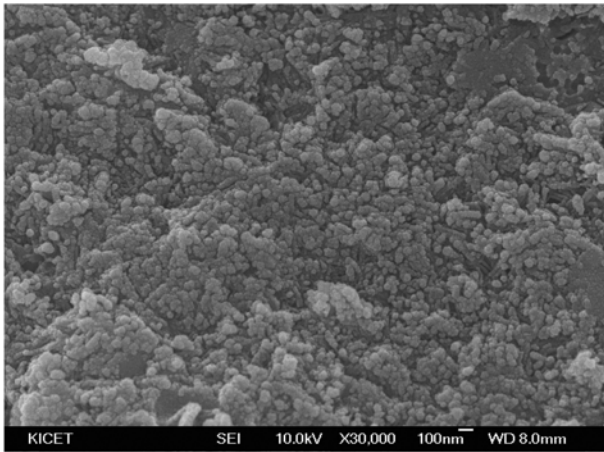


Fig. 9. SEM of the BFS11 hydrate

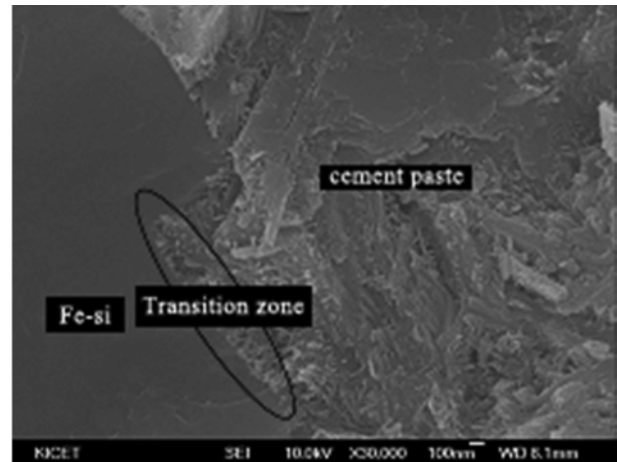


Fig. 11. SEM of the BFS11 hydrate

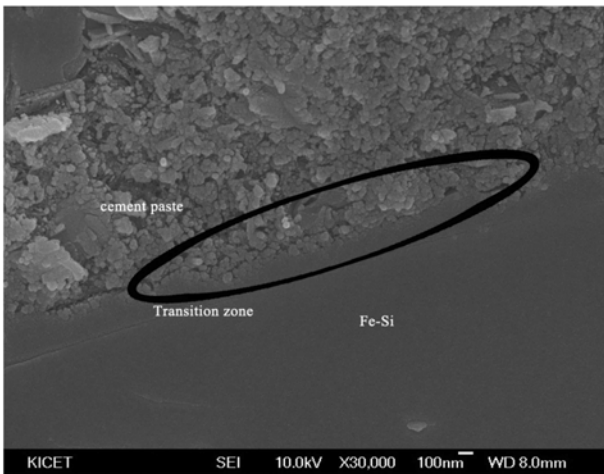


Fig. 10. SEM of the OFS11 hydrate

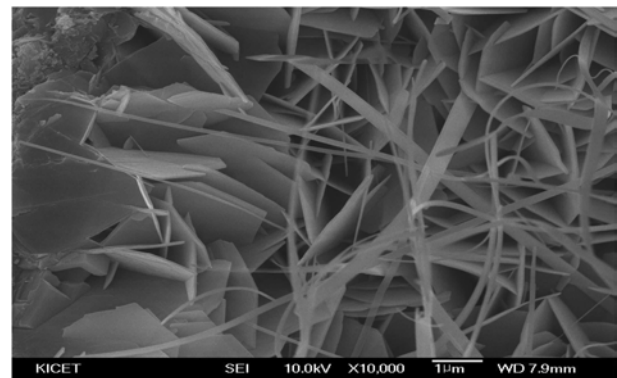


Fig. 12. SEM of tobermorite and zonolite of the BFS11 hydrate

filler [12]. Also, it could be interpreted that hydrates not found in other concrete types might be generated when ferro silicon was cured at high temperature and high pressure, which probably shows a very compact structure exceeding the limitation of current high strength concretes.

Fig. 8 shows an image of OFS11 using ordinary Portland cement and ferro silicon, Fig. 9 shows a view of the internal hydrate of BFS11 using low heat Portland cement and ferro silicon taken by an SEM.

Currently, four types of C-S-H are known; type 1 is fibrous and generally formed in a relatively large volume, type II is glassy, type III is a 10 nm block, and type IV is a block type without any specific features. Fig. 8 shows type 1 OFS11 and type II C-S-H, and Fig. 9 shows type III BFS11 and type IV C-S-H, which seems that the low water-cement ratio from the use of

low heat Portland cement reduces the porosity, inducing the generation of type III and type IV C-S-H, and thus contributing to the improved strength of the compactly hardened structure. The bonding force between aggregates and binder is largely governed by the diameter of aggregates and the macro/microstructures of the transition zone. Comparing Figs. 10 and 11, it is shown that the strength of the BFS11 specimen increased because of the increased transition zone bonding force as the low porous block was filled with C-S-H hydrates. A high temperature facilitates the hydration reaction of cement and activates the pozzolanic reaction, generating tobermorite at temperatures greater than 200 °C [8]. Fig. 12 shows tobermorite and zonolite generated in BFS11, which seems to be attributable to various hydrates when the use of ferro silicon, admixture, and filler facilitates the pozzolanic reaction.

XRD analysis

To examine the substances of hydrates by aggregates and filler through the 250 °C-50 MPa high temperature and high pressure curing, XRD analysis was conducted on the specimens at day 7. Fig. 13 shows that QS11 mainly consists of Si, and contains calcium hydroxide and crystalline illite. Figs. 13~15 show that ferro-silicon was changed into $FeSi_2$ by the high

1. Calcium silicate hydrate is the main product of the hydration of Portland cement and is primarily responsible for the strength in cement based materials.
2. Calcium aluminate hydrate is formed during the hydration of high alumina cement.

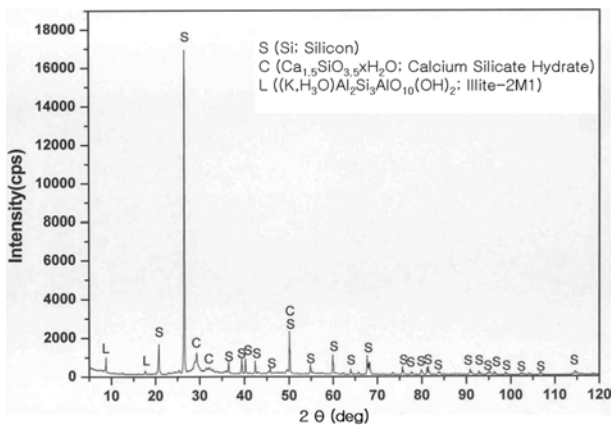


Fig. 13. XRD analysis of the QS11

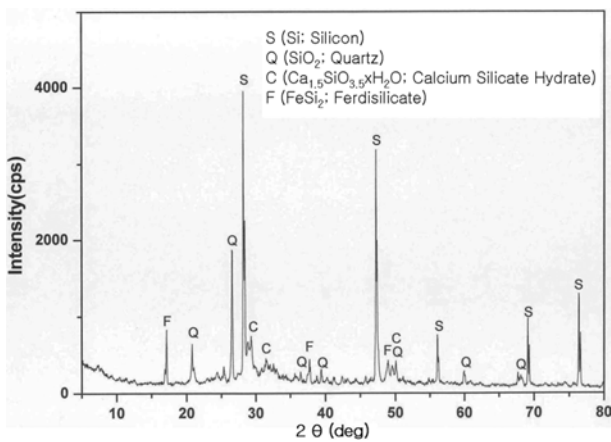


Fig. 14. XRD analysis of the OFS11

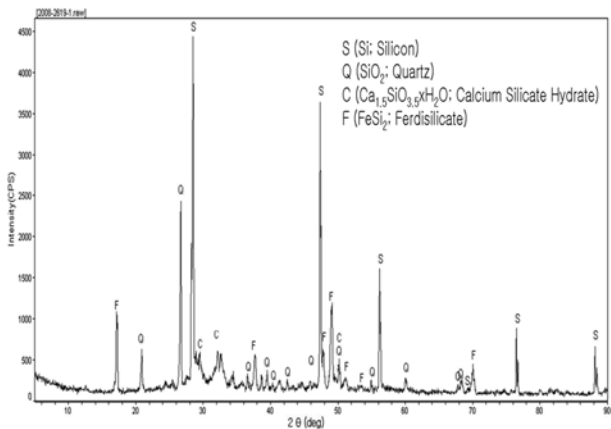


Fig. 15. XRD analysis of the BFS11

temperature and high pressure curing, thus influencing the concrete strength, although its composition is similar to QS11. BFS11 of Fig. 15 shows more hydrates were generated than in OFS11, thereby affecting the strength because it had a higher intensity value although it was similar to OFS11.

Conclusions

This study manufactured ultra-high strength powder concrete by mixing low heat Portland cement, ferro-

silicon, and steel fibers, conducting experiments on the features of materials. The study was ultimately intended to demonstrate the features of ultra-high strength powder concrete using ferro-silicon by means of a compressive strength evaluation, SEM, and XRD analysis. In addition, this study evaluated the compressive strength depending on curing method and times, summarizing with the following conclusions.

1. To develop ultra-high strength powder concrete, coarse aggregate was replaced with 0.6 mm and smaller ferro-silicon, bauxite, dolomite, and silicon, which finally showed that the effect of aggregates on the compressive strength was favorable in the order of: ferro-silicon > bauxite > dolomite > silicon. In addition, it was also found that cement paste was highly strengthened by fine aggregates, compactly filling powder, and the use of reactive materials. Ferro-silicon showed the highest strength when its mixture was 110% on the basis of cement weight.

2. In the case of a specimen using silicon, an SEM comparison showed that a C-S-H gel was independently formed, mutually linked to many hydrates, and had significant $\text{Ca}(\text{OH})_2$ crystals. On the other hand, the ferro-silicon mixed specimen showed significant C-S-H (calcium silicate hydrate paste) in a complicated and compact structure. The ferro-silicon mixed specimen using ordinary Portland cement showed Type I and II C-S-H hydrates, and the ferro-silicon mixed low heat Portland cement specimen showed Type III and IV C-S-H hydrates because of a reduced water-cement ratio.

3. It also showed that a filler supplementing an insufficient silica component and filling pores had the proper input ratio. In addition, it is considered that using ultra-fine powder like silica fume and fine quartz reacts with $\text{Ca}(\text{OH})_2$, generating calcium hydroxide hydrates to fill pores, thus improving the transition zone and finally realizing the ultra-high strength.

4. As a result of compacting the specimen with pressure and curing under a high temperature to achieve a higher strength, the number of large pores was reduced. Moreover, curing under a maintained high temperature and pressure generated tobermorite and zonalite, hydrates generated at 200 °C and higher, which also yielded a higher compressive strength.

5. High strength concrete is largely affected by materials, unlike ordinary concrete. Specifically, special attention should be paid to selecting aggregates, the quality of cement and a high performance water reducing agent, fluidity, admixture, and aggregate. After realizing a high strength concrete mixture design, an ultra-high strength powder concrete yielding greater than 400 MPa could be successfully developed.

Acknowledgements

The authors acknowledge financial support from the Korea Ministry of Construction and Transportation.

References

1. G.T. Ko, J.J. Park, Korea Society of Civil Engineers, 27 [3] (2004) 427-432.
2. S.H. Bae, Korea Concrete Institute Collection of Papers, 15 [3] (2003) 129-133.
3. H. Lim, J.J. Park, Civil Engineering, HanyangUniv, (2008).
4. B.W. Jo, S.G. Park, Advances in Cement Research, 22 [2] (2010) 91-97.
5. H.J. Min, S.J. Lim, Architectural Institute of Korea Collection of Papers. 26 (2006).
6. H.J. Min, U.J. Kim, Architectural Institute of Korea Collection of Papers, 23 [7] (2007).
7. Y.G. Yun, H.S. Yun, The Korean Society of Mechanical Engineers. 24 [12] (2000) 2909-2916.
8. M. Mazloom, A.A. Ramezaniapour, J.J. Brooks, Cement and Concrete Composites, (2003) 12-34.
9. J.J. Park, G.T. Ko, Korea Concrete Institute Collection of Papers, 17 [1] (2003) 35-41.
10. H.Y. Moon, G.Y. Kim, Concrete Institute Collection of Papers, 4 [2] (1992).
11. Richard. P, Cheyrezy. M, Cement and Concrete Research, 25 [7] (1995) 1501-1511.
12. Richard. P, Cheyrezy. M, ACI Spring Convention, 27 [3] (1994) 507-517.
13. A. Palomo, M.W. Grutzeck, M.T. Blanco, Cement and Concrete Research. 29 (1999) 1323-1329.